Geophysical Research Letters

RESEARCH LETTER
10.1029/2021GL096805

Autonomous Wintertime Observations of Air-Sea Exchange in the Gulf Stream Reveal a Perfect Storm for Ocean CO_2 Uptake

S. Nickford[1], J. B. Palter[1], K. Donohue[1], A. J. Fassbender[2], A. R. Gray[3], J. Long[4], A. J. Sutton[2], N. R. Bates[5,6], and Y. Takeshita[4]

[1]Graduate School of Oceanography, University of Rhode Island, Narragansett, RI, USA, [2]NOAA/OAR Pacific Marine Environmental Laboratory, Seattle, WA, USA, [3]School of Oceanography University of Washington, Seattle, WA, USA, [4]Monterey Bay Aquarium Research Institute, Moss Landing, CA, USA, [5]Bermuda Institute of Ocean Sciences, Ferry Reach, Bermuda, [6]Department of Ocean and Earth Sciences, University of Southampton, Southampton, UK

Abstract A scarcity of wintertime observations of surface ocean carbon dioxide partial pressure (pCO_2) in and near the Gulf Stream creates uncertainty in the magnitude of the regional carbon sink and its controlling mechanisms. Recent observations from an Uncrewed Surface Vehicle (USV), outfitted with a payload to measure surface ocean and lower atmosphere pCO_2, revealed sharp gradients in ocean pCO_2 across the Gulf Stream. Surface ocean pCO_2 was lower by ∼50 µatm relative to the atmosphere in the subtropical mode water (STMW) formation region. This undersaturation combined with strong wintertime winds allowed for rapid ocean uptake of CO_2, averaging −11.5 mmol m^{-2} day^{-1} during the February 2019 USV mission. The unique timing of this mission revealed active STMW formation. The USV proved to be a useful tool for CO_2 flux quantification in the poorly observed, dynamic western boundary current environment.

Plain Language Summary The North Atlantic Ocean absorbs more atmospheric carbon dioxide (CO_2) than most regions of the global ocean. Using an ocean drone in the Gulf Stream region during the winter of 2019, we measured the air-sea CO_2 difference, calculated the air-sea CO_2 exchange, and compared our results to previous wintertime ship-based measurements. We find that the region south of the Gulf Stream can absorb vast amounts of atmospheric CO_2, owing both to surface ocean properties and the strong wintertime winds. Because of extremely sparse wintertime observations in this region, we hypothesize that ocean uptake of CO_2 may be underestimated. Our work suggests that ocean drones can help close the observational gaps that create uncertainty in ocean carbon uptake in challenging regions and seasons, if these vehicles and the sensors they carry can be made robust to large breaking waves.

Key Points:

- Surface waters in the subtropical mode water formation region are lower in pCO_2 than in the atmosphere in winter by ∼50 µatm
- Strong wintertime winds drive atmospheric CO_2 into the ocean near the Gulf Stream with high spatial and temporal variability
- Uncrewed surface vehicles provide an opportunity to refine quantification and understanding of CO_2 exchange near western boundary currents

Supporting Information:

Supporting Information may be found in the online version of this article.

Correspondence to:

S. Nickford,
sarah_nickford@uri.edu

Citation:

Nickford, S., Palter, J. B., Donohue, K., Fassbender, A. J., Gray, A. R., Long, J., et al. (2022). Autonomous wintertime observations of air-sea exchange in the Gulf Stream reveal a perfect storm for ocean CO_2 uptake. *Geophysical Research Letters*, *49*, e2021GL096805. https://doi.org/10.1029/2021GL096805

Received 27 OCT 2021
Accepted 28 JAN 2022

Author Contributions:

Conceptualization: J. B. Palter, K. Donohue, A. J. Fassbender, A. R. Gray, A. J. Sutton
Data curation: S. Nickford, A. J. Fassbender, J. Long, A. J. Sutton, N. R. Bates, Y. Takeshita
Formal analysis: S. Nickford
Funding acquisition: S. Nickford, J. B. Palter, K. Donohue, A. J. Fassbender, A. R. Gray, A. J. Sutton
Investigation: S. Nickford, J. B. Palter, K. Donohue, J. Long
Resources: A. J. Fassbender, J. Long, Y. Takeshita
Supervision: J. B. Palter
Visualization: S. Nickford
Writing – original draft: S. Nickford
Writing – review & editing: J. B. Palter, K. Donohue, A. J. Fassbender, A. R.

1. Introduction

1.1. Western Boundary Current Regions Are Hot Spots for CO_2 Uptake

Western Boundary Currents (WBCs), like the Gulf Stream, and their neighboring subtropical mode water (STMW) formation regions are locations of intense heat loss (Marshall et al., 2009) and are thought to have high rates of ocean carbon dioxide (CO_2) uptake (Andersson et al., 2013; Bates et al., 2002; Landschützer et al., 2013; Takahashi et al., 2009). Here, heat and carbon exchange between the ocean and atmosphere is mediated by strong winds. As the surface water cools, the solubility of CO_2 increases, thereby intensifying the difference between atmosphere and surface ocean partial pressure of CO_2 (ΔpCO_2). Additionally, the Gulf Stream transports waters out of the tropics that have a low Revelle factor and are therefore more efficient at absorbing atmospheric CO_2 (Sabine et al., 2004). Thus, the wintertime Gulf Stream region has the ingredients for a "perfect storm" of CO_2 uptake: strong and cold winds, large air-sea pCO_2 gradient, and low Revelle factor.

Despite their potential to act as hot spots of ocean CO_2 uptake, WBC regions have seldom been observed in winter and lack carbon system measurements. One exception is in the North Pacific, where 7 years of measurements from the Kuroshio Extension Observatory surface mooring have shown that the lowest ocean pCO_2 and highest capacity for ocean CO_2 uptake occur in winter (Fassbender et al., 2017). Even in the well-observed North Atlantic, wintertime ocean carbon measurements in the Gulf Stream region have been rare (Bakker et al., 2016). Two research cruises conducted in 2006 and 2007, both part of the US CLIVAR Mode Water Dynamics Experiment (CLIMODE; Andersson et al., 2013), are the only surveys to measure ocean carbon in complete cross-Gulf Stream transects in the wintertime.

Gray, J. Long, A. J. Sutton, N. R. Bates, Y. Takeshita

North Atlantic STMW, also known as 18° Water, is formed on the southeast side of the Gulf Stream (Worthington, 1959). Here, surface cooling creates deep wintertime mixed layers with nearly vertically homogeneous temperature (17.8°–18.4°C), absolute salinity (36.45–36.55 g kg^{-1}), and potential density (σ_θ = 1026.45–1026.55 kg m^{-3}, Andersson et al., 2013; Bates, 2012). At the start of spring, this mixed layer is capped by a warm layer and may be subducted into the main thermocline (Stommel, 1979). The STMW occupies a large volume of water (Forget et al., 2011) with substantial interannual variability in carbon storage rates (Bates, 2012). Due to the limited observations leading up to, during, and after the formation of STMW in the North Atlantic, our understanding of CO_2 dynamics in this region is incomplete.

Uncrewed Surface Vehicles (USVs) can increase observing capacity in WBCs, by reducing the expense associated with ship time and the risk to crew in difficult weather. The Saildrone Explorer is a highly maneuverable USV with an endurance of several months that moves quickly through the water (2–4 kts) and carries a large sensor payload (Supporting Information S1). Saildrones are capable of making the measurements needed to quantify air-sea CO_2 exchange in a variety of challenging environments like the Southern Ocean, as shown by previous studies (such as Meinig et al., 2019; Sabine et al., 2020; Sutton et al., 2021; Zhang et al., 2019).

Here, we analyze and interpret measurements from the deployment of a Saildrone USV equipped with an Autonomous Surface Vehicle CO_2 ($ASVCO_2$™; Sabine et al., 2020) system in the Gulf Stream in February 2019 and a ship-based survey on the R/V *Endeavor* in the subtropical gyre in March 2019. Our objectives were to: (a) collect climate-quality pCO_2 measurements (measurement uncertainty of ocean pCO_2 of <2 µatm; Bender et al., 2002) in the Gulf Stream and surrounding region during winter; (b) quantify air-sea CO_2 fluxes in the Gulf Stream, STMW formation region, and subtropical gyre interior; (c) compare the results to existing pCO_2 and air-sea CO_2 flux data and products; and (d) describe the physical processes that create ocean pCO_2 anomalies.

2. Materials and Methods

2.1. In Situ Data Collection

2.1.1. The Saildrone USV

From 2 to 21 February 2019 the Gulf Stream Saildrone Mission provided continuous ocean and lower atmosphere temperature and pCO_2 data (Figure 1), among a suite of additional variables (Text S1 in Supporting Information S1). With each Gulf Stream crossing, we aimed to occupy a transect extending at least 10 km beyond the Gulf Stream to both the north and the south. The center of the Gulf Stream is identified as the depth-averaged velocity maximum (Halkin et al., 1985), and the Gulf Stream's northern and southern edges are defined by the 0 m s^{-1} isotachs. In total, the USV crossed the Gulf Stream center five times.

Ocean and atmosphere pCO_2 were measured hourly by the $ASVCO_2$, which performs a two-point calibration before measuring each sample. Ocean pH was measured by a Honeywell Durafet at 10-min intervals. Because of the sharp gradients and rich spatial structures associated with the Gulf Stream, we use the higher-resolution pH data to infill the gaps between hourly directly measured pCO_2 measurements. Moreover, the pH sensor persisted in taking measurements for 24 hr after a storm damaged the $ASVCO_2$ system. Therefore, we calculate pCO_2 from the pH data using a regional total alkalinity-salinity relationship (Equation S1 in Text S2 in Supporting Information S1) in CO2sys, which is a carbonate system calculator (Lewis & Wallace, 1998). The drift of the pH sensor was corrected by subtracting the 12-hr running mean of the offset between the directly measured pCO_2 data and the calculated pCO_2 (see Figure S1 and Text S2 in Supporting Information S1), after which the calculated and directly measured pCO_2 closely match (r = 0.87, RMSE = 3.85 µatm). Hereafter, we use pCO_2 calculated from the 10-min pH data; the qualitative results and interpretation are unchanged if we used the directly measured pCO_2 for the time that both sensors were operating.

Over the entire mission, wind speeds averaged 9.4 ± 4.3 m s^{-1} (mean ± standard deviation; 18.3 ± 8.4 kts), with daily average maximums reaching 21 m s^{-1} (40.8 kts) due to four substantial storms in which the central pressures plunged as low as 960 hPa and significant wave heights peaked at 7 m. During a fifth storm, the $ASVCO_2$ and pH sensors stopped functioning, ending data collection for those sensors on February 20 and 21, respectively. This slowly moving storm built up the sea state, producing significant wave heights of 12.6 m that damaged the USV wing on 26 February 2019, bringing the mission to an early end.

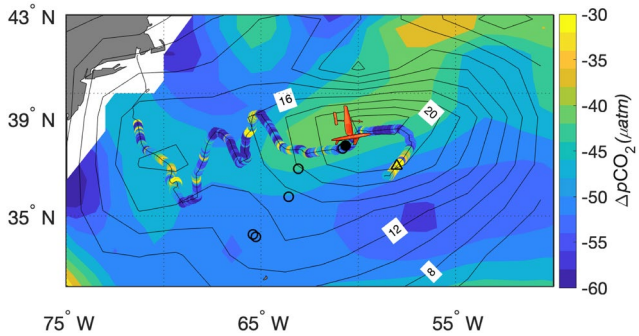

Figure 1. Wind speed (black contours, m s^{-1}) and along-USV-track ΔpCO_2 (dots) plotted on mean February 2019 ΔpCO_2 (shaded background) from the Landschützer et al. (2020) product (referred to as L20). Wind speeds are from 6-hourly NCEP reanalysis on 2/18/2020 at 18:00:00, during a strong storm. The USV position at the time of the plotted winds is shown by the Saildrone icon (icon reproduced from https://www.saildrone.com/technology). Black open circles show the locations of Argo profiles (vertical profiles shown in Figure 4a) with the nearest profile to the USV shown as a filled black circle. The black open triangle shows the location where the USV encountered subtropical mode water (STMW) formation.

2.1.2. R/V *Endeavor*

A planned rendezvous between the R/V *Endeavor* and the USV was rerouted after the storm damaged the USV sensors. Instead, the cruise sampled in calmer conditions northwest of Bermuda from 27 February 4 March 2019 (Figure 2). In addition to the ship's Conductivity-Temperature-Depth (CTD), Acoustic Doppler Current Profiler (ADCP), and meteorological sensors, *Endeavor* was equipped with a pH sensor (Deep-Sea-Durafet; Johnson et al., 2016) attached to the underway seawater intake (5 m depth) that sampled every 15 s. The pH data, on the total scale at *in situ* temperature, were calibrated with 17 discrete pH samples, which were also analyzed for dissolved inorganic carbon (DIC) and total alkalinity (TA; Text S3 in Supporting Information S1).

2.1.3. The CLIMODE Program

The CLIMODE Program supported five cruises from 2005 to 2007 in the North Atlantic STMW formation region (Marshall et al., 2009). The second CLIMODE cruise (CLIMODE-2) took place from 18 to 31 January 2006 and was the only cruise to take continuous underway carbon system data, while it zig-zagged across the Gulf Stream for a total of 10 Gulf Stream crossings.

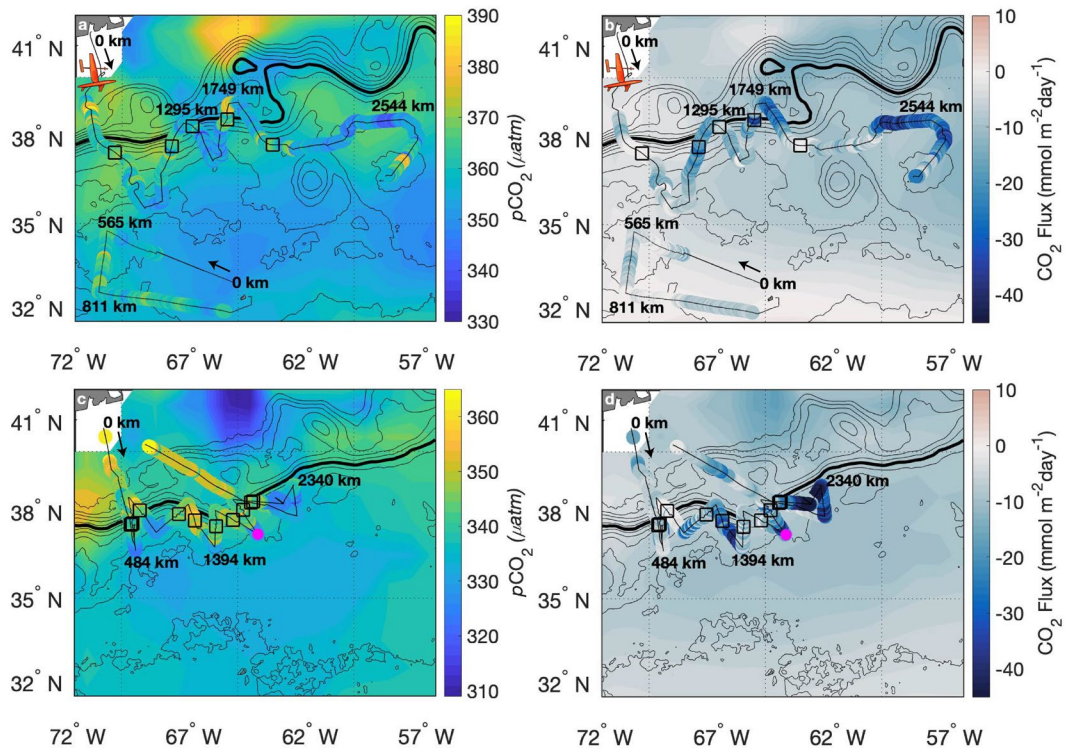

Figure 2. Ocean pCO_2 (left) and air-sea CO_2 flux (right; negative numbers indicate ocean carbon uptake). Top panels show the February 2019 L20 ocean pCO_2 and air-sea CO_2 flux in color shading with data from the Uncrewed Surface Vehicle (USV) 2 to 21 February 2019 mission and R/V *Endeavor* 27 February 4 March 2019 cruise as dots along their respective tracks. Bottom panels show the same but for the January 2006 L20 and the second CLIVAR Mode Water Dynamics Experiment (CLIMODE-2) 18–31 January 2006 cruise track. Cumulative along-track distances are labeled in km with an arrow (at 0 km) indicating direction of the platform. Black contours show the average sea surface temperature (SST) for the respective month of the cruise from satellite GHRSST at 1°C intervals with the 18°C isotherm in bold (indicating the mean position of the Gulf Stream). The open squares indicate the location of the Gulf Stream center at the time of crossing and the magenta circle in the bottom panels indicates the location of the CTD cast featured in Figure 4c.

The ship collected surface data via a thermosalinograph and Submersible Autonomous Moored Instrument pCO_2 sensor (SAMI-CO_2), and occupied CTD sections on five crossings. The SAMI-CO_2 was connected to the ship's underway seawater intake line (4 m) and sampled every 15 min, with calibrations provided by discrete DIC and TA samples (Andersson et al., 2013, Text S4 in Supporting Information S1). Atmospheric pCO_2 was not measured on the ship and is therefore taken from the weekly Tudor Hill Marine Atmospheric Observatory observations in Bermuda.

3. Results and Discussion

3.1. Low Ocean pCO_2 Measured in STMW *Precursor* Waters

As the CLIMODE-2 and USV missions proceeded from west to east over the course of a few winter weeks, data show progressive cooling of SSTs. For example, Figure 3b shows the USV measurements south of the Gulf Stream cooling from 20°C to 18°C from along-track distance 750 km to 2,800 km (approximately 69°W to 58°W). Similarly, Figure 3f shows CLIMODE-2 cruise measurements south of the Gulf Stream cooling from 20°C to 19°C from along-track distance 400–2,200 km (approximately 69°W to 63°W).

Cooling of seawater in isolation would cause a pCO_2 decline due to the thermodynamic effect. Equation 1 is typically applied to help interpret the pCO_2 seasonal cycle (Takahashi et al., 1993, 2002). Here, we use it to explore how cooling of Gulf Stream waters influences surface pCO_2 on the south side of the Gulf Stream, under the assumption that these waters are effectively recirculating Gulf Stream waters (see Brambilla & Talley, 2006):

$$pCO_2^T = pCO_2^{GS} \times \exp\left[0.0423\ (T - T_{GS})\right], \quad (1)$$

where pCO_2^T is the predicted pCO_2 due to ocean cooling, pCO_2^{GS} is the mean pCO_2 observed within the Gulf Stream, $T-T_{GS}$ is the anomaly from the mean Gulf Stream SST. The data reveal this simple framework, which seems to explain the SST-pCO_2 relationship above 20°–21°C (black solid lines in Figures 4b and 4d), albeit with considerable scatter. This relationship appears to change sign at ∼20°C, for which a hypothesized mechanism is proposed in Section 3.2.

The pCO_2 minimum is found in the STMW precursor waters, which are those surface waters south of the Gulf Stream that are cool relative to the Gulf Stream but reside above the seasonal thermocline and have the potential to be transformed to STMW in late winter under continued cooling (Figures 4a and 4c). The distinct pCO_2 minimum in STMW precursor waters is most visually apparent in CLIMODE-2 (Figures 2c and 2d; Figures 3e and 3f), which consistently sampled well to the south of the Gulf Stream. The low pCO_2 in STMW precursor waters leads to strong ocean CO_2 uptake in the STMW formation region: -11.5 mmol m^{-2} day^{-1} during the USV mission, and -20.0 mmol m^{-2} day^{-1} during CLIMODE-2 (Text S5 in Supporting Information S1). In both cases large fluxes were driven by strong winds (Table 1).

In Figures 2 and 3 and Table 1, we compare measured pCO_2 from USV, *Endeavor*, and CLIMODE-2 surveys to an annually updated, monthly ocean pCO_2 estimate created byLandschützer et al. (2016) version 2020 (referred to as L20). This product is constructed by relating measured ocean pCO_2 from the Surface Ocean CO_2 Atlas to predictor variables, such as mixed layer depth and SST from satellite observations or ocean reanalysis products, using a neural network approach (Landschützer et al., 2016). For this analysis, we use the 2020 version of L20, which did not include the 2019 USV measurements in its training data set (https://doi.org/10.7289/V5Z899N6). We interpolate the L20 ocean pCO_2 field for the month and year of observations to the location of each observation. The monthly L20 surface ocean pCO_2 product agrees with the measured values (Table 1). However, its 1° horizontal resolution hides the spatial gradients captured by *in situ* observations in the Gulf Stream region. Moreover, L20 does not capture the pCO_2 minimum in the STMW formation region, where difference between observations and L20 are largest, likely due to the lack of wintertime training data and coarse spatial resolution of the L20 product (Table 1; Figure 2). Given that this region has strong winds in winter and the air-sea CO_2 flux is dependent on the squared wind speed (Equations S2 and S3 in Text S5 in Supporting Information S1), air-sea fluxes are maximized here, and a pCO_2 bias can have a large impact on the calculated flux. In contrast, during the *Endeavor* cruise, the L20 ocean pCO_2 product is in close agreement with the observations collected in the Sargasso Sea (Figures 2a and 3c; Table 1), possibly a result of the more spatially homogeneous conditions.

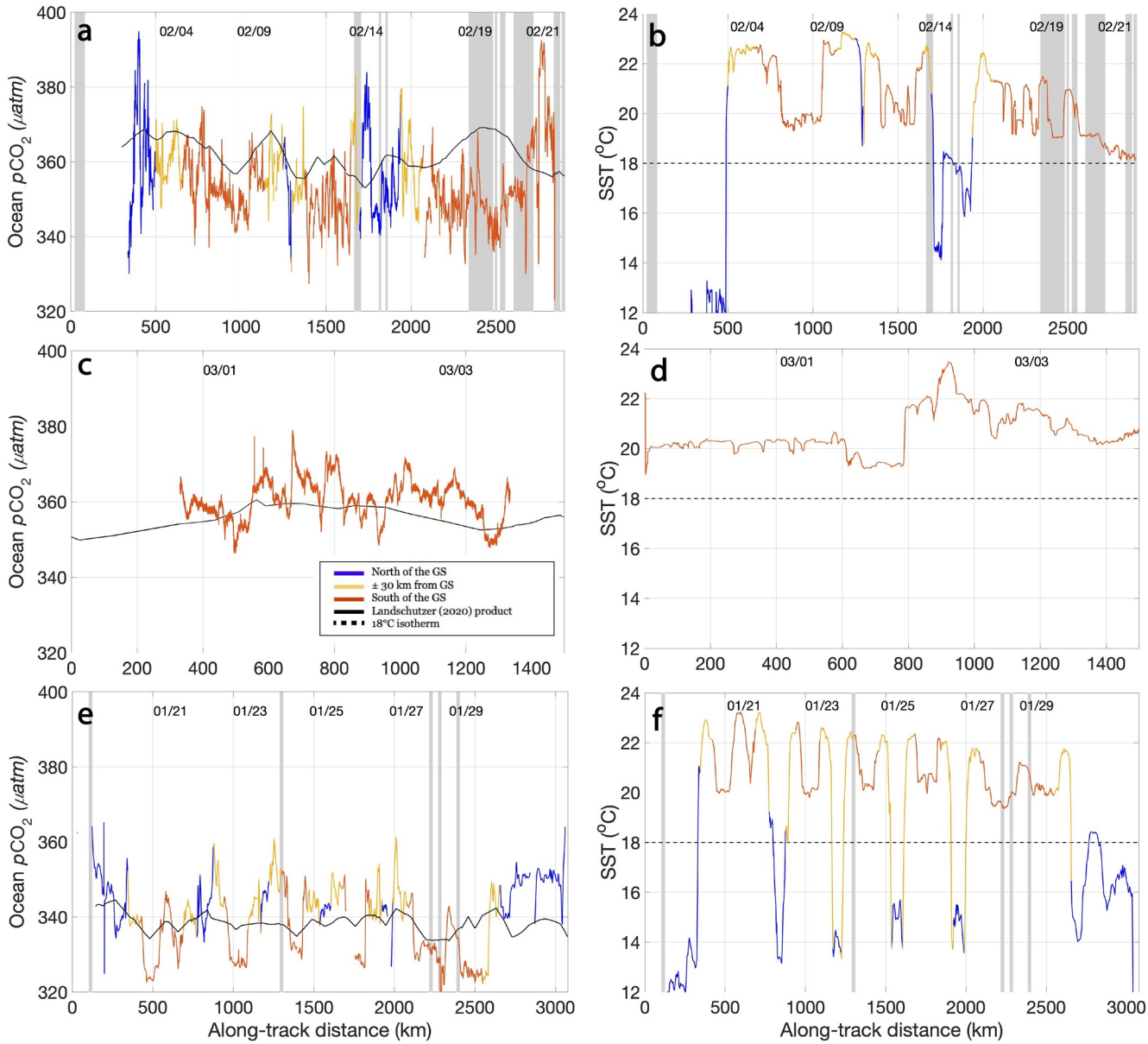

Figure 3. Ocean pCO_2 and sea surface temperature (SST) as a function of distance along the uncrewed surface vehicle (USV), R/V *Endeavor*, and CLIVAR Mode Water Dynamics Experiment (CLIMODE)-2 missions. (left) Ocean pCO_2, with periods of hourly averaged wind speed >15 m s^{-1} highlighted in gray, and (right) SST during (a–b) USV, (c–d) R/V *Endeavor,* and (e–f) CLIMODE-2 cruises. The 18°C isotherm is shown as a black dashed line on right hand panels. Line color indicates the position of the measurement relative to the Gulf Stream (as indicated in the legend in panel c). The black line in each panel on the left shows the L20 pCO_2 product for the appropriate month linearly interpolated to the position of the USV or ship (Landschützer et al., 2020; version 2020). Dates corresponding to along-track distances are shown at the top of each panel (month/day).

3.2. Autonomous Observations of Active STMW Formation

STMW formation occurs when strong wintertime surface heat loss on the equatorward side of the Gulf Stream creates deep, vertically homogeneous mixed layers (300–500 m) with a temperature of ∼18°C (Stevens et al., 2020). At the end of the winter, these surface waters cool enough to mix past the seasonal thermocline. The CLIMODE-2 cruise was too early in winter to sample STMW formation, as surface ocean temperatures were well above 18°C and mixed layer depths were less than 200 m (Figures 4c and 4d).

We infer that the USV briefly encountered active STMW formation (location marked by black open triangle in Figure 1) on 21 February, 1 day after a storm with 15 m s^{-1} mean wind speeds and air temperatures of 9°C passed

Table 1
Surface Properties and Fluxes Averaged Over the Observational Period When the Platform (Research Vessel or Uncrewed Surface Vehicle [USV]) Was Within 30 km of the Gulf Stream (GS) Center or to its South

Observational mission	Location relative to GS	Ocean pCO_2 (μatm)	RMSE[a] and *MSD* for L20 minus observations for ocean pCO_2	Atm pCO_2 (μatm) (data source[b])	ΔpCO_2 (μatm)	Wind speed[c] (m s^{-1}) *variance*	CO_2 flux[d] (mmol m^{-2} day^{-1})
USV (Saildrone) (February 2019)	GS	357.5	**9.2**	405.4 ($ASVCO_2$ on Saildrone)	−48.1	**8.6**	−8.8
			3.7			*30.1*	
	South	352.4	**13.6**	403.0 ($ASVCO_2$ on Saildrone)	−50.8	**9.9**	−11.5
			9.2			*20.1*	
Endeavor (March 2019)	South	360.5	**5.5**	404.4 (Tudor Hill)	−43.9	**7.5**	−6.4
			−2.8			*8.3*	
CLIMODE-2 (January 2006)	GS	343.8	**7.5**	378.8 (Tudor Hill)	−35.1	**11.9**	−11.7
			−4.3			*25.9*	
	South	331.8	**8.7**	378.8 (Tudor Hill)	−47.1	**13.9**	−20.0
			4.7			*24.5*	

[a]Root Mean Squared Error (RMSE) and Mean Signed Deviation (MSD) are computed from the monthly L20 data (from the same month as the corresponding mission), interpolated along the route of the ship or USV. [b]Because some missions did not measure atmospheric pCO_2, we indicate the data source for each row, with Tudor Hill referring to the Tudor Hill Marine Atmospheric Observatory in Bermuda interpolated to the time of the ocean pCO_2 observations (Dlugokencky et al., 2021). [c]Wind speed was measured on the research vessels and USV, adjusted to 10 m height when necessary, and reported as averages for the periods when the USV or ships were in or south of the Gulf Stream. [d]CO_2 fluxes are calculated from wind speeds, ocean pCO_2 measured or calculated from pH contemporaneously on ships or the USV, and the atmospheric pCO_2 listed in this table, with details provided in Text S5 in Supporting Information S1.

over the region. The inference of deep vertical mixing into the permanent thermocline was made by comparing the SST measured by the USV to a nearby Argo float profile. The closest Argo profile to the USV path (6.3 km and 12 hr apart) is highlighted in Figure 4a, with its location indicated in Figure 1. Three days after the Argo profile was collected, the USV first measured surface temperatures of 18.5°C, consistent with mixing past the seasonal thermocline. The float profile shows that this surface temperature was previously found at a depth of 520 m and capped by the seasonal thermocline (Figure 4a, purple line and dot). Therefore, SSTs at and below 18.5°C measured by the USV were likely the signature of vertical convective mixing to a depth of at least 500 m (Andersson et al., 2013). In these cold surface waters, ocean pCO_2 was measured at the highest levels south of the Gulf Stream (>380 µatm; Figure 4b). These cold waters showed considerable pCO_2 variability, as would be expected if patchy convective mixing were bringing to the surface remineralized DIC that had accumulated in the vestigial STMW layer. We define vestigial STMW as the STMW formed in a previous year that has been recirculating beneath the seasonal thermocline. We estimate the DIC of the vestigial STMW to be 2119.3 ± 9.3 µmol kg^{-1} (Texts S6 and S7 in Supporting Information S1). The SST-pCO_2 relationship for waters below ~20°C can likely be explained by this DIC-rich subsurface water mixing toward the surface during STMW formation (Figure 4b).

4. Conclusions

This work shows vigorous uptake of atmospheric CO_2 in the STMW formation region, both from traditional ship-based and state-of-the-art autonomous measurements. In both wintertime surveys, ocean pCO_2 is lowest to the south of the Gulf Stream in cool waters that have not yet mixed below the seasonal thermocline to become STMW (Table 1). Here, ocean CO_2 uptake is maximized, with influxes of 11.5–20.0 mmol m^{-2} day^{-1} due to the strong winds and large ocean-atmosphere pCO_2 difference of ~−50 µatm. Therefore, the cold, strong winds create the "perfect storm" for ocean CO_2 uptake in the STMW precursor waters that are low in ocean pCO_2 before the vertical mixing of vestigial STMW brings DIC-rich waters to the surface and reduces the CO_2 flux into the ocean.

The spatial average from an empirical reconstruction of surface ocean pCO_2 (L20) is in close agreement with the observations presented here (Table 1). However, relative to the USV and CLIMODE-2 observations, the L20 product misses the large undersaturation of STMW precursor waters, which will lead to low biases in the ocean CO_2 uptake in this region. It is possible that overcoming the scarcity of wintertime measurements in this challenging region could remedy this issue, with USVs feasibly offering a key tool to make these observations.

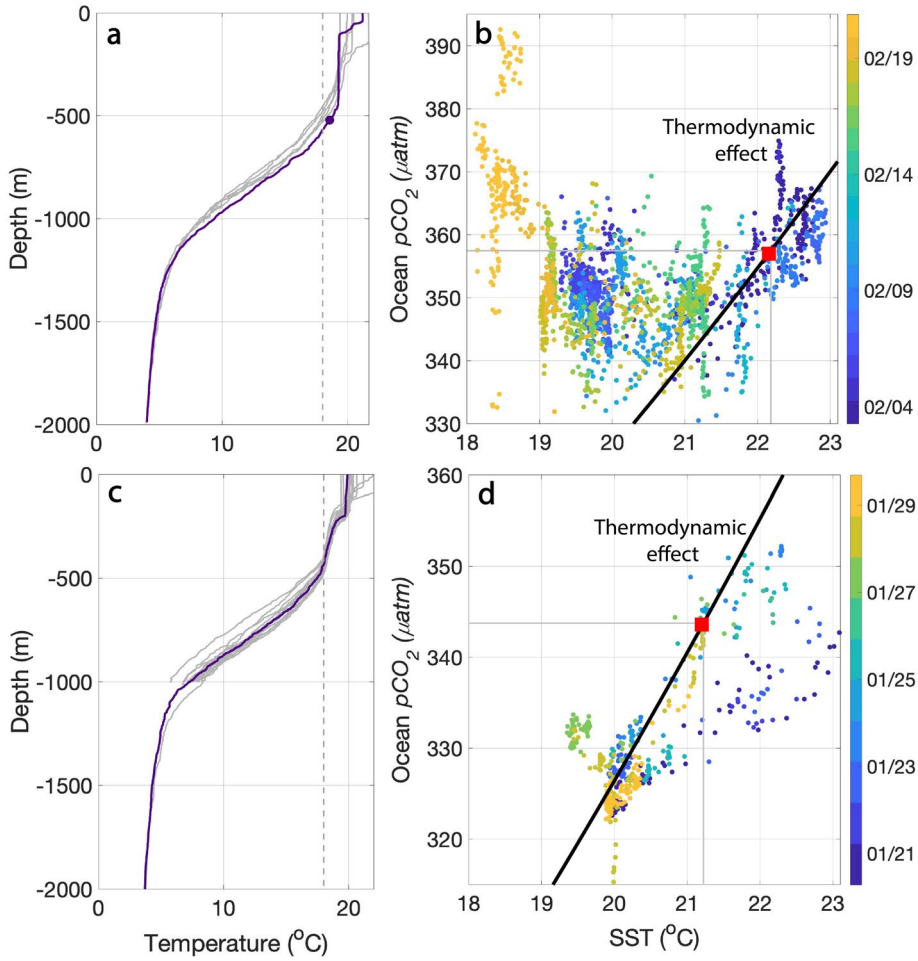

Figure 4. pCO_2 versus sea surface temperature (SST) observed during the Uncrewed Surface Vehicle (USV) and CLIVAR Mode Water Dynamics Experiment (CLIMODE) missions, and the inferred role of cooling versus vertical mixing. (a) Argo profiles collected in the subtropical mode water (STMW) formation region during February 2019 (gray traces) and a profile collected 12 hr before the USV passed by (purple trace; geographical location of profiles can be found in Figure 1). The purple dot indicates the cold SST measured by the USV near the profile. The 18°C isotherm is marked with a dashed gray line as a reference. (b) Scatterplot of USV-observed ocean pCO_2 versus SST for data collected south of the Gulf Stream, colored by time (month/day). The black solid line shows the thermodynamic effect (Equation 1). The red square shows the average SST and ocean pCO_2 in the Gulf Stream during the mission, used in the calculation (Equation 1). (c) CTD profiles collected during the CLIMODE-2 cruise, following the same color scheme as (a), where the location of the representative profile can be found in Figure 2 (magenta circle). (d) Same as in panel (b) but for CLIMODE-2 observations.

The STMW sets the memory of the subtropics because it records the previous winter's conditions, allowing these properties to be reexposed in the following winter. Thus, an interesting question remains open: What is the fate of the CO_2 absorbed in the STMW formation region? Lagrangian modeling studies suggest STMW contributes to the northward limb of the Atlantic Meridional Overturning Circulation (AMOC, Burkholder & Lozier, 2014). Therefore, CO_2 uptake during STMW formation may feed anthropogenic carbon into the AMOC deep limb upon its densification at higher latitudes (Iudicone et al., 2016). If the annually integrated surface CO_2 fluxes in the STMW formation region were higher than the STMW DIC accumulation rate, it would provide support for this conceptual model in which CO_2 taken up in STMW is exported from the subtropical gyre. Sustained measurements of air-sea CO_2 exchange in the Gulf Stream and STMW formation region would provide a means to compare STMW CO_2 uptake with DIC accumulation rates directly measured at BATS, as well as with observations collected by the rapidly proliferating array of Biogeochemical-Argo floats.

Data Availability Statement

The Data from the USV mission are available at https://doi.org/10.25921/2dw3-d527. The data from the CLIMODE program are available at http://sam.ucsd.edu/ltalley/climode_ctdhydro/index.html. R/V *Endeavor* cruise data can be found at https://doi.org/10.7284/908397. The L20 product is available for download at https://doi.org/10.7289/V5Z899N6.

Acknowledgments
The authors gratefully acknowledge thoughtful reviews from Rik Wanninkhof and an anonymous reviewer, whose feedback significantly improved this manuscript. This work was funded by NSF RAPID award #1850608, the Saildrone Award, the Rhode Island Endeavor Program, and the Rhode Island Space Grant Graduate Fellowship Award. The authors acknowledge Stacy Maenner for her contribution to data processing and thoughtful advice, and Marguerite Blum for analyzing the discrete DIC, TA, and pH samples. They gratefully acknowledge the crew of the R/V *Endeavor*. A. J. Fassbender was supported by NOAA's Global Ocean Monitoring and Observing Program. A. R. Gray was supported by NOAA through award NA20OAR4320271. This is PMEL contribution 5282.

References

Andersson, A. J., Krug, L. A., Bates, N. R., & Doney, S. C. (2013). Sea-air CO_2 flux in the North Atlantic subtropical gyre: Role and influence of sub-tropical mode water formation. *Deep-Sea Research Part II Topical Studies in Oceanography*, *91*, 57–70. https://doi.org/10.1016/j.dsr2.2013.02.022

Bakker, D. C. E., Pfeil, B., Landa, C. S., Metzl, N., O'Brien, K. M., Olsen, A., et al. (2016). A multi-decade record of high-quality fCO_2 data in version 3 of the Surface Ocean CO_2 Atlas (SOCAT). *Earth System Science Data*, *8*(2), 383–413. https://doi.org/10.5194/essd-8-383-2016

Bates, N. R. (2012). Multi-decadal uptake of carbon dioxide into subtropical mode water of the North Atlantic Ocean. *Biogeosciences*, *9*(7), 2649–2659. https://doi.org/10.5194/bg-9-2649-2012

Bates, N. R., Pequignet, A. C., Johnson, R. J., & Gruber, N. (2002). A short-term sink for atmospheric CO_2 in subtropical mode water of the North Atlantic Ocean. *Nature*, *420*(6915), 489–493. https://doi.org/10.1038/nature01253

Bender, M., Doney, S., Feely, R. A., Fung, I., Gruber, N., Harrison, D. E., et al. (2002). A large-scale CO_2 observing plan: In situ oceans and atmosphere (LSCOP). *In Situ large-scale CO_2 observations working group*. Retrieved from https://www.globalcarbonproject.org/global/pdf/lscop2002.pdf

Brambilla, E., & Talley, L. D. (2006). Surface drifter exchange between the North Atlantic subtropical and subpolar gyres. *Journal of Geophysical Research*, *111*(7), 1–16. https://doi.org/10.1029/2005JC003146

Burkholder, K. C., & Lozier, M. S. (2014). Tracing the pathways of the upper limb of the North Atlantic meridional overturning circulation. *Geophysical Research Letters*, *41*(12), 4254–4260. https://doi.org/10.1002/2014GL060226

Dlugokencky, E. J., Mund, J. W., Crotwell, A. M., Crotwell, M. J., & Thoning, K. W. (2021). *Atmospheric carbon dioxide dry air mole fractions from the NOAA GML carbon cycle cooperative global air sampling network, 1968-2020, version: 2021-07-30*. https://doi.org/10.15138/wkgj-f215

Fassbender, A. J., Sabine, C. L., Cronin, M. F., & Sutton, A. J. (2017). Mixed-layer carbon cycling at the Kuroshio extension observatory. *Global Biogeochemical Cycles*, *31*(2), 272–288. https://doi.org/10.1002/2016GB005547

Forget, G., Maze, G., Buckley, M., & Marshall, J. (2011). Estimated seasonal cycle of North Atlantic eighteen degree water volume. *Journal of Physical Oceanography*, *41*(2), 269–286. https://doi.org/10.1175/2010JPO4257.1

Halkin, D., Rossby, H. T., & Rossby, T. (1985). Structure and transport of the gulf stream at 73 N. *Journal of Physical Oceanography*. https://doi.org/10.1175/1520-0485(1985)015<1439:TSATOT>2.0.CO;2

Iudicone, D., Rodgers, K. B., Plancherel, Y., Aumont, O., Ito, T., Key, R. M., et al. (2016). The formation of the ocean's anthropogenic carbon reservoir. *Scientific Reports*, *6*, 1–16. https://doi.org/10.1038/srep35473

Johnson, K. S., Jannasch, H. W., Coletti, L. J., Elrod, V. A., Martz, T. R., Takeshita, Y., et al. (2016). Deep-Sea DuraFET: A pressure tolerant PH sensor designed for global sensor networks. *Analytical Chemistry*, *88*(6), 3249–3256. https://doi.org/10.1021/acs.analchem.5b04653

Landschützer, P., Gruber, N., & Bakker, D. C. E. (2016). Decadal variations and trends of the global ocean carbon sink. *Global Biogeochemical Cycles*, *30*(10), 1396–1417. https://doi.org/10.1002/2015GB005359

Landschützer, P., Gruber, N., & Bakker, D. C. E. (2020). An observation-based global monthly gridded sea surface pCO2 product from 1982 onward and its monthly climatology (NCEI Accession 0160558), Version 5.5 [Dataset]. NOAA National Centers for Environmental Information. https://doi.org/10.7289/V5Z899N6

Landschützer, P., Gruber, N., Payne, M. R., Schuster, U., Bakker, D. C. E., Nakaoka, S., et al. (2013). A neural network-based estimate of the seasonal to inter-annual variability of the Atlantic Ocean carbon sink. *Biogeosciences*, *10*(11), 7793–7815. https://doi.org/10.5194/bg-10-7793-2013

Lewis, E., & Wallace, D. (1998). Program developed for CO_2 system calculations. *ORNL/CDIAC-105*. Retrieved from http://cdiac.esd.ornl.gov/oceans/co2rprtnbk.html

Marshall, J., Andersson, A., Bates, N., Dewar, W., Doney, S., Edson, J., et al. (2009). The CLIMODE field campaign observing the cycle of convection and restratification over the gulf stream. *Bulletin of the American Meteorological Society*, *90*(9), 1337–1350. https://doi.org/10.1175/2009BAMS2706.1

Meinig, C., Burger, E. F., Cohen, N., Cokelet, E. D., Cronin, M. F., Cross, J. N., et al. (2019). Public private partnerships to advance regional ocean observing capabilities: A saildrone and NOAA-PMEL case study and future considerations to expand to global scale observing. *Frontiers in Marine Science*, *6*, 1–15. https://doi.org/10.3389/fmars.2019.00448

Sabine, C., Sutton, A., McCabe, K., Lawrence-Slavas, N., Alin, S., Feely, R., et al. (2020). Evaluation of a new carbon dioxide system for autonomous surface vehicles. *Journal of Atmospheric and Oceanic Technology*, *37*(8), 1305–1317. https://doi.org/10.1175/JTECH-D-20-0010.1

Sabine, C. L., Feely, R. A., Gruber, N., Key, R. M., Lee, K., Bullister, J. L., et al. (2004). The oceanic sink for anthropogenic CO_2. *Science*, *305*(5682), 367–371. https://doi.org/10.1126/science.1097403

Stevens, S. W., Johnson, R. J., Maze, G., & Bates, N. R. (2020). A recent decline in North Atlantic subtropical mode water formation. *Nature Climate Change*, *10*. https://doi.org/10.1038/s41558-020-0722-3

Stommel, H. (1979). Determination of water mass properties of water pumped down from the Ekman layer to the geostrophic flow below. *Proceedings of the National Academy of Sciences*, *76*(7), 3051–3055. https://doi.org/10.1073/pnas.76.7.3051

Sutton, A. J., Williams, N. L., & Tilbrook, B. (2021). Constraining Southern Ocean CO_2 flux uncertainty using uncrewed surface vehicle observations. *Geophysical Research Letters*, *48*(3). https://doi.org/10.1029/2020gl091748

Takahashi, T., Olafsson, J., Goddard, J. G., Chipman, D. W., & Sutherland, S. C. (1993). Seasonal variation of CO_2 and nutrients in the high latitude surface oceans: A comparative study. *Global Biogeochemical Cycles*, *7*(4), 843–878. https://doi.org/10.1029/93gb02263

Takahashi, T., Sutherland, S. C., Sweeney, C., Poisson, A., Metzl, N., Tilbrook, B., et al. (2002). Global sea-air CO_2 flux based on climatological surface ocean pCO_2, and seasonal biological and temperature effects. *Deep-Sea Research Part II Topical Studies in Oceanography*, *49*, 1601–1622. https://doi.org/10.1016/S0967-0645(02)00003-6

Takahashi, T., Sutherland, S. C., Wanninkhof, R., Sweeney, C., Feely, R. A., Chipman, D. W., et al. (2009). Climatological mean and decadal change in surface ocean pCO_2, and net sea-air CO_2 flux over the global oceans. *Deep-Sea Research Part II Topical Studies in Oceanography*, *56*(8–10), 554–577. https://doi.org/10.1016/j.dsr2.2008.12.009

Worthington, L. V. (1959). The 18° water in the Sargasso Sea. *Deep-Sea Research*, *5*(2–4), 297–305. https://doi.org/10.1016/0146-6313(58)90026-1

Zhang, D., Cronin, M. F., Meinig, C., Thomas Farrar, J., Jenkins, R., Peacock, D., et al. (2019). Comparing air-sea flux measurements from a new unmanned surface vehicle and proven platforms during the spurs-2 field campaign. *Oceanography*, *32*(2), 122–133. https://doi.org/10.5670/oceanog.2019.220

References From the Supporting Information

Cai, W.-J., Hu, X., Huang, W.-J., Wang, Y., Peng, T.-H., & Zhang, X. (2010). Alkalinity distribution in the western North Atlantic Ocean margins. *Journal of Geophysical Research*, *115*. https://doi.org/10.1029/2009jc005482

Carter, B. R., Radich, J. A., Doyle, H. L., & Dickson, A. G. (2013). An automated system for spectrophotometric seawater pH measurements. *Limnology and Oceanography: Methods*, *11*(1), 16–27. https://doi.org/10.4319/lom.2013.11.16

Clayton, T. D., & Byrne, R. H. (1993). Spectrophotometric seawater pH measurements: Total hydrogen ion concentration scale calibration of m-cresol purple and at-sea results. *Deep-Sea Research Part I Oceanographic Research Papers*, *40*(10), 2115–2129. https://doi.org/10.1016/0967-0637(93)90048-8

Dickson, A. G., Afghan, J. D., & Anderson, G. C. (2003). Reference materials for oceanic CO_2 analysis: A method for the certification of total alkalinity. *Marine Chemistry*, *80*(2–3), 185–197. https://doi.org/10.1016/S0304-4203(02)00133-0

Dickson, A. G., Sabine, C. L., & Christian, J. R. (2007). *Guide to best practices for ocean CO_2 measurements*. PICES Special Publication.

Dickson, A. G., Wesolowski, D. J., Palmer, D. A., & Mesmer, R. E. (1990). Dissociation constant of bisulfate ion in aqueous sodium chloride solutions to 250°C. *Journal of Physical Chemistry*, *94*(20), 7978–7985. https://doi.org/10.1021/j100383a042

Garcia, H., Weathers, K. W., Paver, C. R., Smolyar, I., Boyer, T. P., Locarnini, R. A., et al. (2018). *World ocean Atlas 2018. Volume 4: Dissolved inorganic nutrients (phosphate, nitrate and nitrate+nitrite, silicate)* (p. 35). NOAA Atlas NESDIS.

Lauvset, S. K., Lange, N., Tanhua, T., Bittig, H. C., Olsen, A., Kozyr, A., et al. (2021). An updated version of the global interior ocean biogeochemical data product. *Earth System Science Data*, *13*, 1–32. https://doi.org/10.5194/essd-12-3653-2020

Lueker, T. J., Dickson, A. G., & Keeling, C. D. (2000). Ocean *p*CO2 calculated from dissolved inorganic carbon, alkalinity, and equations for K1 and K2: Validation based on laboratory measurements of CO_2 in gas and seawater at equilibrium. *Marine Chemistry*, *70*(1–3), 105–119. https://doi.org/10.1016/S0304-4203(00)00022-0

Martz, T. R., Connery, J. G., & Johnson, K. S. (2010). Testing the Honeywell Durafet® for seawater pH applications. *Limnology and Oceanography: Methods*, *8*(MAY), 172–184. https://doi.org/10.4319/lom.2010.8.172

Schmidt, K. M., Swart, S., Reason, C., & Nicholson, S. A. (2017). Evaluation of satellite and reanalysis wind products with in situ wave glider wind observations in the southern ocean. *Journal of Atmospheric and Oceanic Technology*, *34*(12), 2551–2568. https://doi.org/10.1175/JTECH-D-17-0079.1

Sutton, A. J., Sabine, C. L., Maenner-Jones, S., Lawrence-Slavas, N., Meinig, C., Feely, R. A., et al. (2014). A high-frequency atmospheric and seawater pCO_2 data set from 14 open-ocean sites using a moored autonomous system. *Earth System Science Data*, *6*, 353–366. https://doi.org/10.5194/essd-6-353-2014

Takeshita, Y., Johnson, K. S., Martz, T. R., Plant, J. N., & Sarmiento, J. L. (2018). Assessment of autonomous pH measurements for determining surface seawater partial pressure of CO_2. *Journal of Geophysical Research: Oceans*, *123*(6), 4003–4013. https://doi.org/10.1029/2017JC013387

Uppström, L. R. (1974). The boron/chlorinity ratio of deep-sea water from the Pacific Ocean. *Deep-Sea Research and Oceanographic Abstracts*, *21*(2), 161–162. https://doi.org/10.1016/0011-7471(74)90074-6

Wanninkhof, R. (2014). Relationship between wind speed and gas exchange over the ocean revisited. *Limnology and Oceanography: Methods*, *12*(JUN), 351–362. https://doi.org/10.4319/lom.2014.12.351

Wanninkhof, R., Zhang, J.-Z., Baringer, M. O., Langdon, C., Cai, W.-J., Salisbury, J. E., & Byrne, R. H. (2016). Partial pressure (or fugacity) of carbon dioxide, dissolved inorganic carbon, pH, alkalinity, temperature, salinity and other variables collected from discrete sample and profile observations using CTD, bottle and other instruments from NOAA Ship RONALD H. BROWN in the Gray's Reef National Marine Sanctuary, Gulf of Mexico and North Atlantic Ocean from 2012-07-21 to 2012-08-13 (NCEI accession 0157619). [surface alkalinity and salinity] [Dataset]. NOAA National Centers for Environmental Information. https://doi.org/10.3334/cdiac/otg.coastal_gomecc2

Weiss, R. F. (1974). Carbon dioxide in water and seawater: The solubility of a non-ideal gas. *Marine Chemistry*, *2*, 203–215. https://doi.org/10.1016/0304-4203(74)90015-2